Advances in Concrete Construction, *Vol. 3, No. 4 (2015) 269-282*
DOI: http://dx.doi.org/10.12989/acc.2015.3.4.269

A new approach for measurement of anisotropic tensile strength of concrete

Vahab Sarfarazi*[1], Hamid R. Faridi[2a], Hadi Haeri[3b] and Wulf Schubert[4]

[1]Department of Mining Engineering, Hamedan University of Technology, Hamedan, Iran
[2]Department of materials science and metallurgy, Hamedan University of Technology, Hamedan, Iran
[3]Post doctoral fellow in Civil Engineering, Department of Civil Engineering, Sharif University of Technology, Member of National Elites Foundation, Tehran,Iran
[4]Institu for Rock Mechanic and Tunnelling, Graz University of Technology, Austria

(Received November 3, 2015, Revised December 27, 2015, Accepted January 14, 2016)

Abstract. In this paper, a compression to tensile load converter device was developed to determine the anisotropic tensile strength of concrete. The samples were made from a mixture of water, fine sand and cement, respectively. Concrete samples with a hole at its center was prepared and subjected to tensile loading using the compression to tensile load converter device. A hydraulic load cell applied compressive loading to converter device with a constant pressure of 0.02 MPa per second. Compressive loading was converted to tensile stress on the sample because of the overall test design. The samples have three different configurations related to loading axis; 0, 45°, -45°. A series of finite element analysis were done to analyze the effect of hole diameter on stress concentration of the hole side along its horizontal axis to provide a suitable criterion for determining the real tensile strength of concrete. Concurrent with indirect tensile test, Brazilian test and three point loading test were also performed to compare the results from the three methods. Results obtained by this device were quite encouraging and show that the tensile strengths of concrete were similar in different directions because of the homogeneity of bonding between the concrete materials. Also, the indirect tensile strength was clearly lower than the Brazilian test strength and three point loading test.

Keywords: compression to tensile load converter device; CTT; anisotropic tensile strength of concrete

1. Introduction

Tensile strength of concrete is of prime importance in case of water retaining structures, runway slabs, pre-stressed concrete members, bond and shear failure of reinforced concrete members and cracking of mass concrete works. Therefore, many experimental and theoretical studies have been carried out to determine the tensile strength of concrete (Zhou 1988, Larrard 1992, Zheng 2001, Gomez 2001, Mier 2002, Zain 2002, Calixto 2002, Swaddiwudhipong 2003,

*Corresponding author, Ph.D., E-mail: Sarfarazi@hut.ac.ir
[a]Ph.D., E-mail: faridihr@hut.ac.ir
[b]Ph.D., E-mail: haerihadi@gmail.com

http://www.techno-press.org/?journal=acc&subpage=7 ISSN: 2234-0912 (Print), 2234-179X (Online)

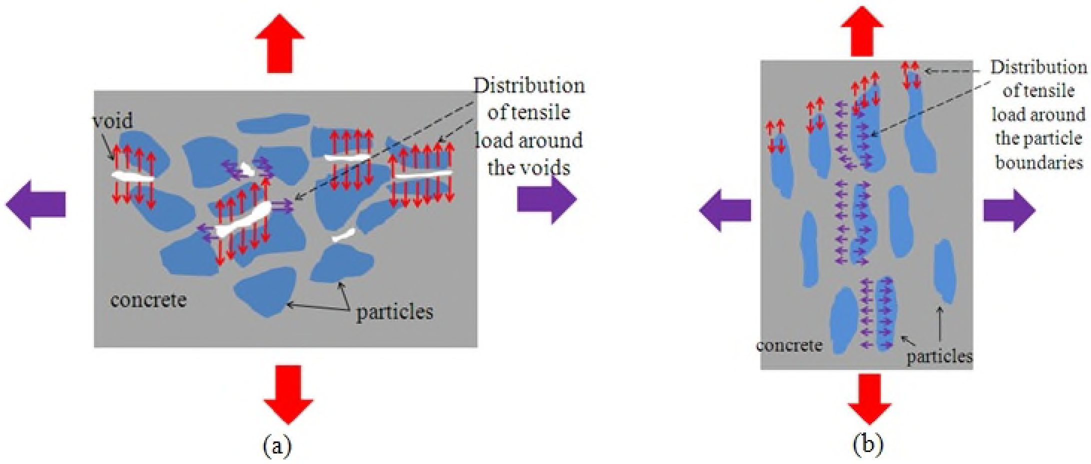

Fig. 1 The anisotropic tensile strength of concrete due to, (a) non-homogeneity of bonding between concrete materials, (b) accumulation of weak plane in special direction

Kim 2014, Mobasher 2014, Tiang 2015, Wan Ibrahim 2015, Silva 2015, Gerges 2015, Liu 2015).

Tensile strength of concrete will be different in various directions due to non-homogeneity of bonding between concrete materials (Fig. 1(a)). Also, accumulation of weak plane in special direction led to anisotropy of tensile strength of concrete (Fig. 1(b)).

The objective of this paper is to develop a new loading device called compression-to-tension converter (CTT) to apply tensile stress to the concrete specimen in different directions. The proposed device will be designed and fabricated for use with most commercially available compression loading machines. It should be durable, inexpensive and easy to use.

2. Experimental and numerical studies

The objective of the laboratory testing was to determine the anisotropic tensile strength of concrete specimen and to assess the performance of the CTT device. Numerical simulation was performed for better understanding of the stress distribution in the model.

The discussions of this chapter were divided to four sections. The first section is describing the technique of preparing the specimens, the second section is focused on the testing procedure in loading the specimens and considering the general experimental observations, the third section describe the procedure of numerical simulation and fourth section discusses the experimental and numerical results.

2.1 The technique in preparation of the internally holed specimens

The concrete specimens were prepared from a mixture of two parts water, one part fine sand, and two parts cement in a blender (Fig. 2(a)). crushed-limestone sand with 2.57 g/cm^3 of specific gravity and 2.75 cm^2/g of fineness was used as fine aggregate. The sieve analyses of the fine aggregates (sand) are given in Table 1. The mixture was then poured into a fiberglass cast with internal dimension of 15×19×6 cm (Fig. 2(b)). The cast consists of two discrete cubes,

Table 1 Grading of sand

Screen size (mm)	Sand (% passing)
9.5	100
4.75	97
2.36	91
1.18	65.8
0.6	46.2
0.3	21.1
0.15	2.5

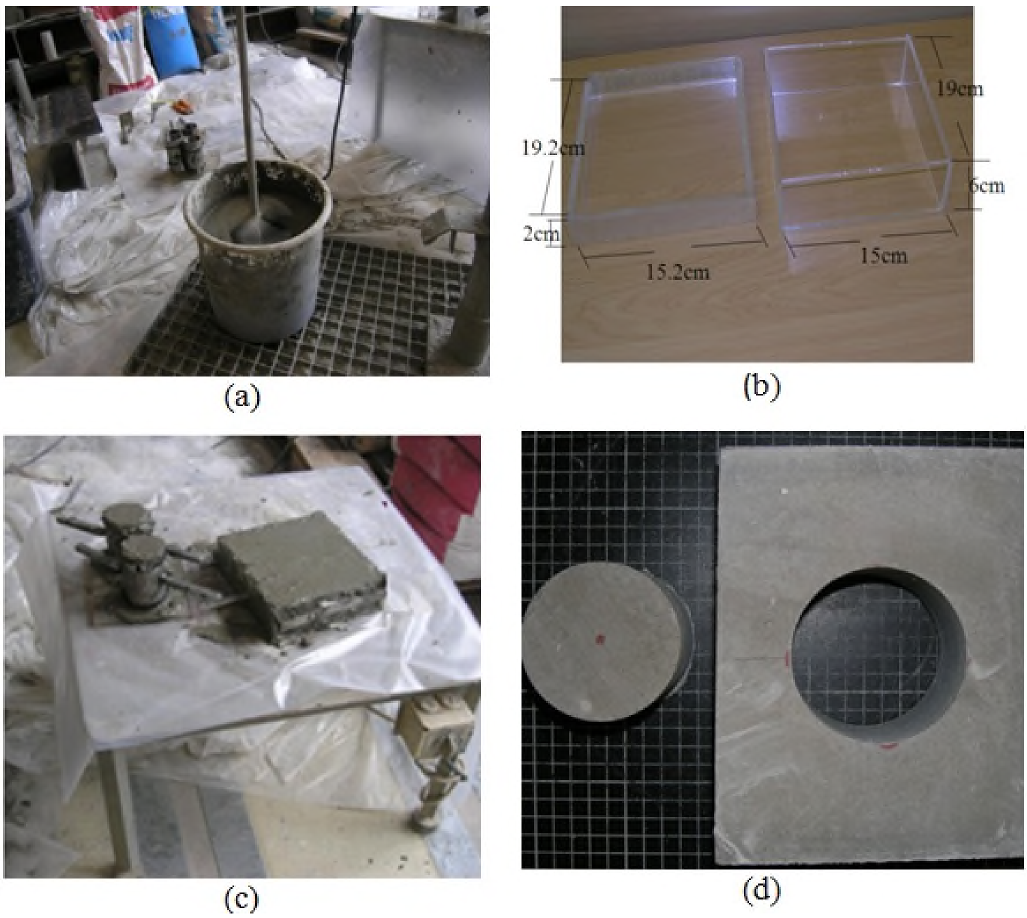

Fig. 2 The technique in preparing the internally hole specimens; (a) mixing materials in a blender, (b) a fiberglass cast, (c) the fresh mixture is vibrated and (d) drilling a core from the Centre of the cubic sample

bolted together. The cast containing fresh mixture was vibrated (Fig. 2(c)) and then stored at room temperature for 8 h afterward, the specimens unmolded. Then a core with diameter of 7.5 cm and height of 60 cm remove from the center of the samples using dry drilling (Fig. 2(d)) so the ratio of hole diameter (7.5 cm) to sample width (15 cm) was 0.5. From each configuration describing above, three similar samples were prepared and were tested under indirect tensile load.

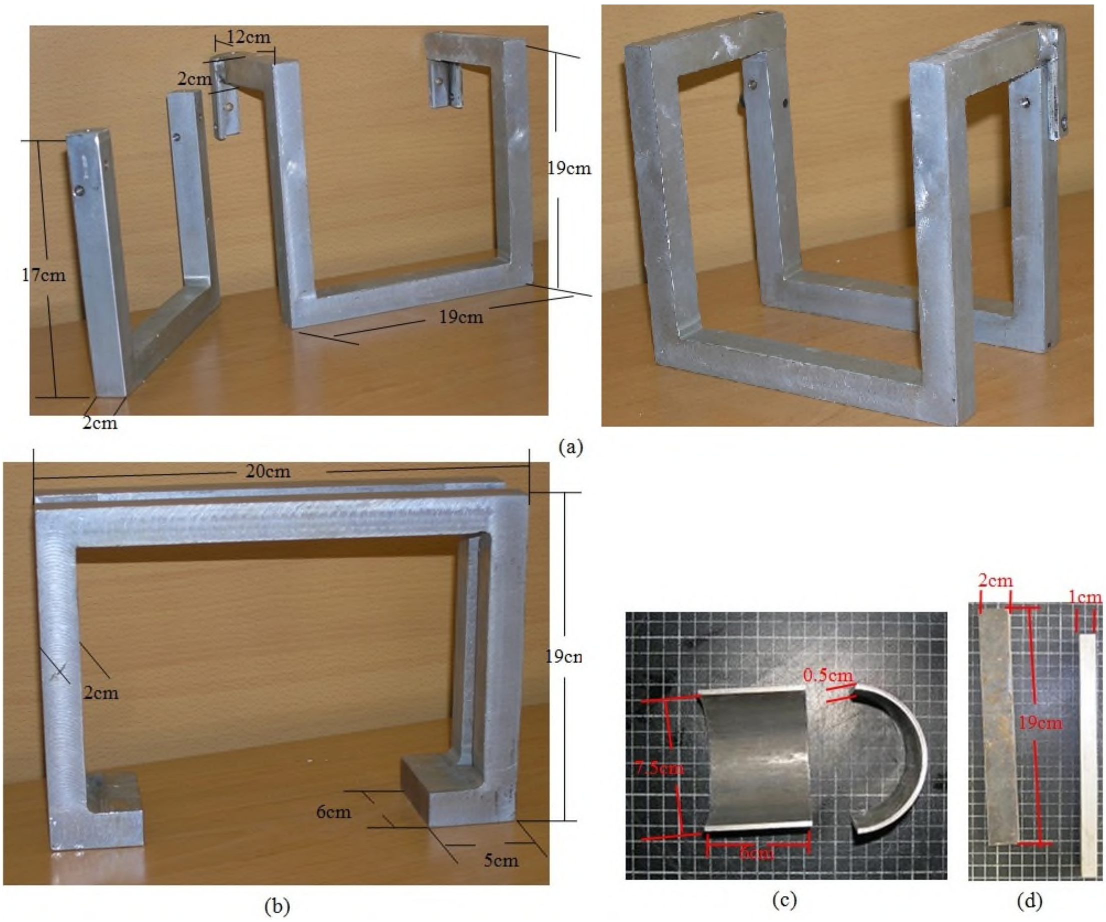

Fig. 3 The components of compression to tension load device

The disc samples for Brazilian test (BS1881 - 117, 1983) and columnar samples for three point loading test (BS1881 - 118, 1983**)** were also prepared to compare the results with those of indirect tension test and in order to control the variability of material. The specimens for Brazilian test were 54 mm in diameter and 27 mm thick. The specimens for three point loading test were 1000 mm in length and 250 mm thick.

2.2 Compression-to-tension load converter devices

A compression-to-tension load transformer device (CTT) was developed to determine the tensile strengths of specimens with a hole in the middle. The primary design requirement is to allow alternating between the application of tensile load and compressive load on the same specimen while placed in conventional compression equipment. The compression-to-tension load transformer device comprises of four parts made from hardened stainless (Fig. 3). Part No. 1 is composed of two pieces as shown in Fig. 3(a). The front view of both pieces is “n” shaped and the side views look like “I” and “L” on the left and right, respectively (Fig. 3(a)). Part No. 2 is one piece and its front view is U shaped (Fig. 3(b)) and the side views look like “Π”. The dimensions

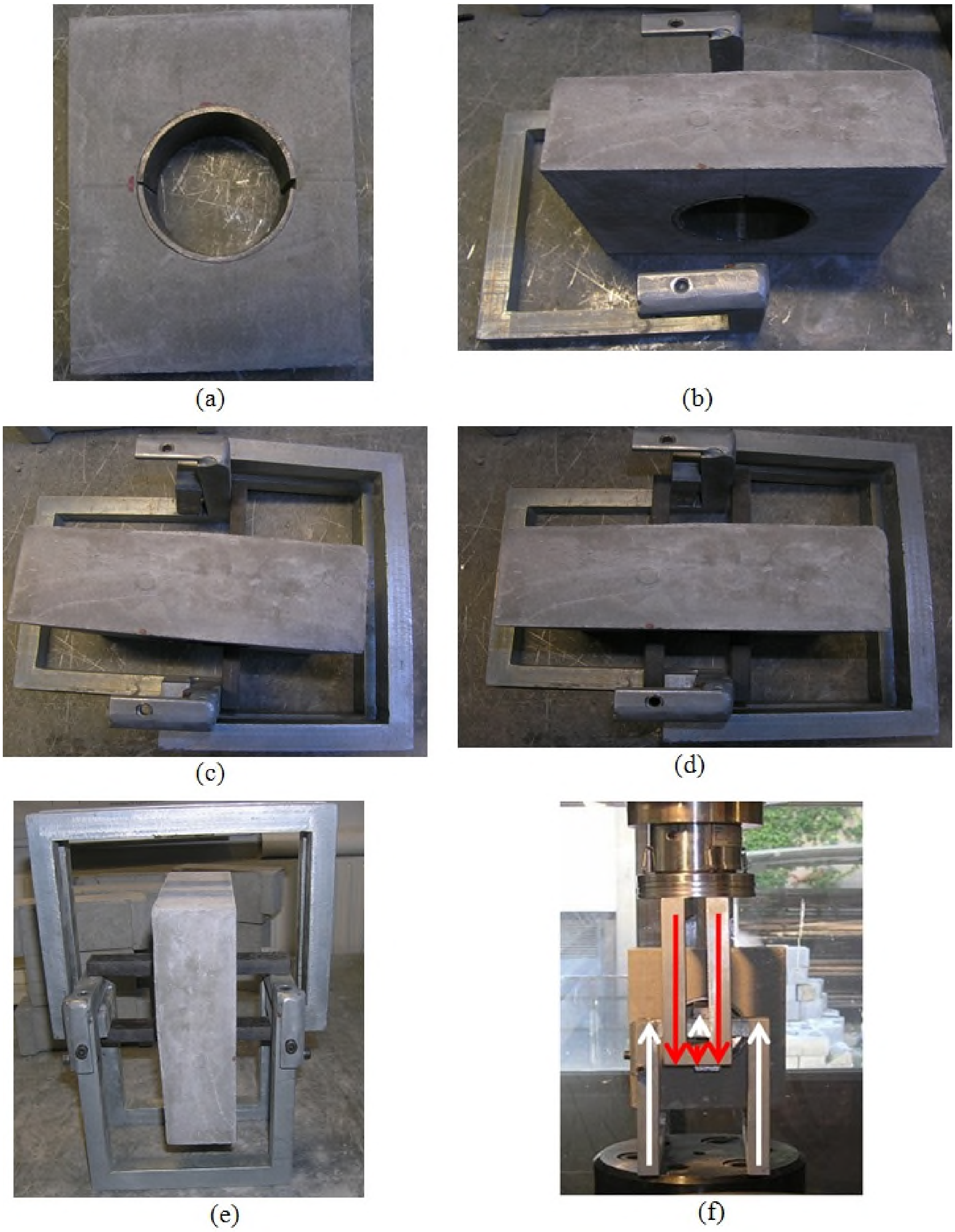

Fig. 4 The set up procedure of CTT device

of the pieces are shown on the Figure. Part No. 3 includes two semi cylindrical stainless steel sleeves, 7.5 cm in diameter, 6 cm long and 1 cm thick as shown in Fig. 3(c). Part No. 4 is composed of two similar 2 cm wide, 19 cm long and 1 cm thick steel blocks (Fig. 3(d)).

The set up procedure of CTT device consists of six stages, as shown in Fig. 4.

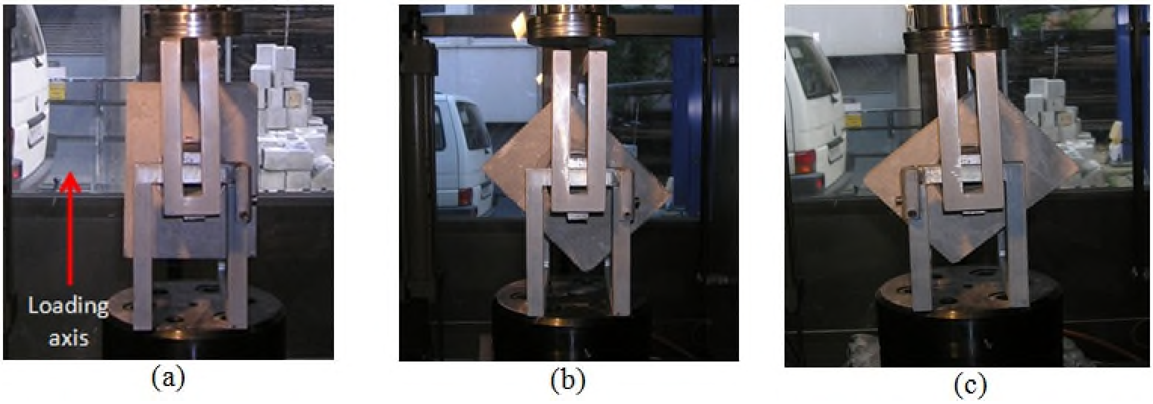

Fig. 5 the vertical side of sample was (a) parallel to the loading axis, (b) returned 45° non counter clock wise related to the loading axis, (c) is returned 45° counter clock wise related to the load axis

1) The two stainless steel sleeves (Part No. 3) are inserted into the hole as shown in Fig. 4(a).

2) With the block laid vertically along its length, the “L” shape segment of Part No. 1 is placed on the left side of the specimen (Fig. 4(b)).

3) One of the steel blocks (Part no. 4) goes through the hole with its upper surface contacting the cylindrical sleeve and its lower surface contacting the “L” shape segment (Fig. 4(c)).

4) Part No. 2 is then placed on the right side of specimen (Fig. 4(c)).

5) The second steel block goes through the hole with its lower surface in contact with cylindrical sleeve and its upper surface contacts with the “Π” shape segment, i.e. part number 2 (Fig. 4(d)).

6) The apparatus assembly is completed when the “I” shaped segment is screwed to the “L” shaped segment of Part No. 1, and the system is set in upright position (Fig. 4(e)).

Under this assembly, the upper part of the concrete block (upper sleeve) is in contact with the lower part of the device and the lower part of the block (lower sleeve) is in contact with the upper part of the device (Fig. 4(e)). When the system is situated between the uniaxial loading frames (as shown In Fig. 4(f)), the upper loading frame compresses the steel sleeve against the lower part of the hole (i.e., pushes the lower part of the slab). Similarly, the lower loading frame pushes the steel block upward against the sleeve, which pushes up the upper part of block. As a resulting of applying the forces is opposite directions, the tensile strength of the device is measured.

By rotating the specimen inside the CTT device, the tensile load was applied to the samples in different directions. Three different configurations were investigated i.e. the vertical side of sample is parallel to the loading axis, the vertical side of sample is returned 45° non counter clock wise related to the loading direction and the vertical side of sample is returned 45° counter clock wise related to tensile load direction (Fig. 5).

2.3 Tensile strength test procedure

Fig. 6 shows test arrangement for indirect tensile strength testing. The CTT device with a specimen was installed in a compression load frame (Fig. 6).

A 30-ton hydraulic load cell applied compressive load to the CTT end plates. An electronic load cell was used to measure the increase of applied loading. To isolate the effect of loading rate

Fig. 6 compression load frame

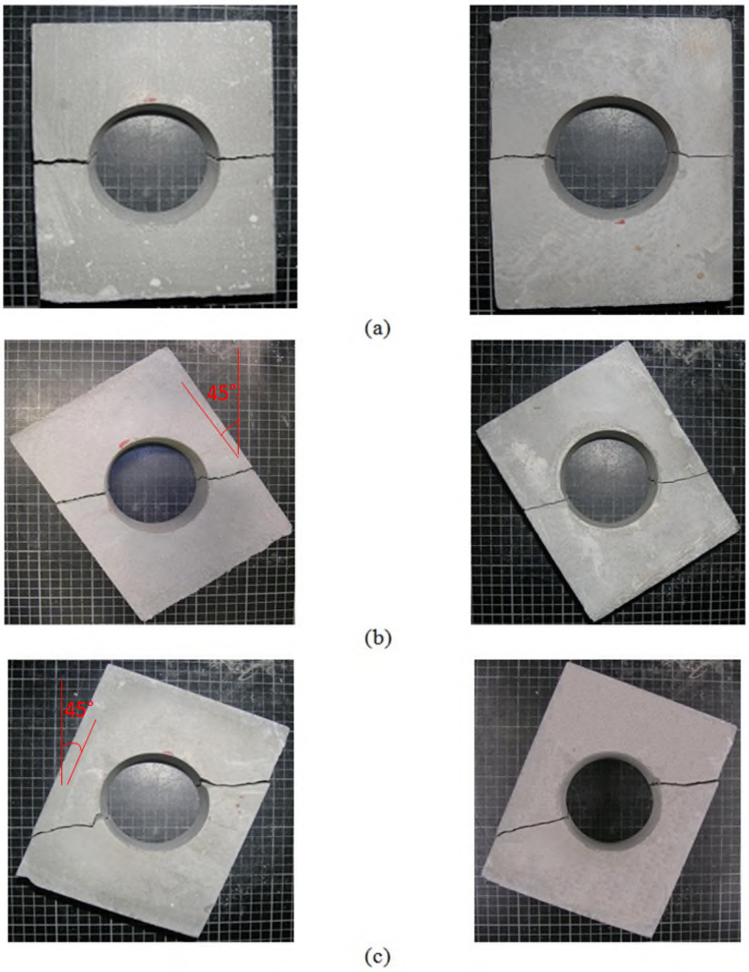

Fig. 7 The tensile failure pattern in samples

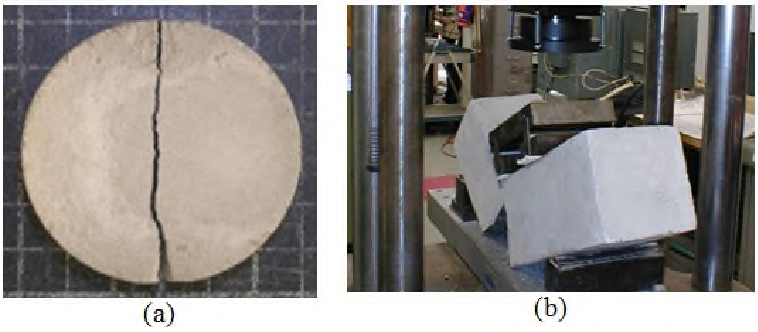

Fig. 8 tensile failure of specimens in, a) Splitting test and b) three point load test

from the results, a constant loading of 0.02 MPa/s was applied for all specimens. The rate was within the range recommended for the Brazilian tensile strength testing by ASTM. From each configuration, two similar samples were prepared and tested under direct tensile test. Totally, Six laboratory tests were performed to assess the performance of CTT device for determining the anisotropic tensile failures of similar concrete slabs. All specimens tested using CTT, cracked along a horizontal line through the center of the hole when subjected to a vertical force. The failure was a splitting tensile failure because the failure happened intentionally along the horizontal axis with the help of two sleeves (Fig. 7). In fact by usage of two semi-circle stainless steels in the hole, stress distribution on top and bottom of the hole was compressive while the stress at the sides of the hole along the horizontal axis was tension. In this condition, the failure under tensile loading occurs at the mid-length before failure by shear stress occurs at both ends of specimen. The analysis of failure pattern and tensile strength is simple by this sleeves configuration. If dimension of sleeves were decreased, the stress was concentrated in some places inside the hole and analysis of failure pattern and tensile strength was difficult.

Three Brazilian tension tests and three point load test were performed to compare the results with those of indirect tension tests. Figs. 8a and b shows the tensile failure of specimen in Splitting test and three point load test, respectively.

2.4 Experimental measurements

The two blades are in contact with the sleeves along their edges. Therefore, the tensile loading on the slab was applied along the 2×6 cm of the edges on top and bottom of the sleeves (Fig. 9). We think it would be practical to calculate the tensile stress along the 12 cm length on each sleeve which is considered being a point loading (stress). For calculating far field tensile stress, the applied loading should be divided to 2×6 cm. The far filed tensile stress is defined as the stress applied to the lines on each blade in connection with the sleeve (Fig. 9). The far field stress at failure causes relatively higher stress concentration on both sides of the hole's wall along the horizontal axes (according to the Kirsch solution (Brady 2006)). Therefore, we need to determine the concentration stress numerically which caused the failure. This concentration stress can be used as ultimate tensile strength of sample.

2.5 Finite element simulation

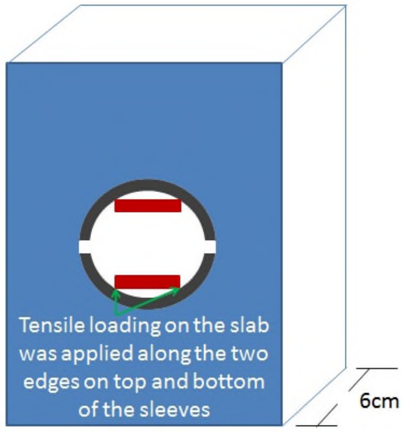

Fig. 9 Tensile loading on the slab was applied along the 2×6 cm of the edges on top and bottom of the sleeves

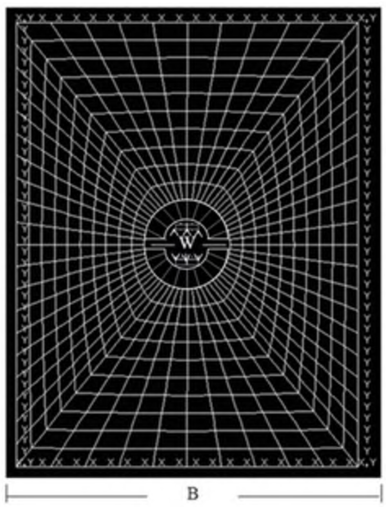

Fig. 10 Finite element mesh with boundary and loading conditions

Numerical simulations also were performed to analyze the stress distributions in the model and determine the real tensile strength of material. The numerical simulation is necessary to determine a relationship between the far field failure stress, the ratio of hole diameter to sample width and the stress concentration on the edges of the hole along the horizontal axis. Output of numerical simulation is a criterion which gives the real tensile strength of concrete.

A two-dimensional finite element code named FRANC2D/L (FRacture ANalysis Code for 2-D Layered structures) was used to perform the numerical modelling work. This code, which was originally developed at Cornell University and modified for multi-layers at Kansas State University, is based on the theory of linear and nonlinear elastic fracture mechanics (Wawrzynek and Ingraffea, (Wawrzynek 1987)). The general methodology starts with the pre-processing stage, where the geometry, mesh, material properties, and boundary conditions are specified. The modelling continues with post-processing stage where loading conditions, crack definition and

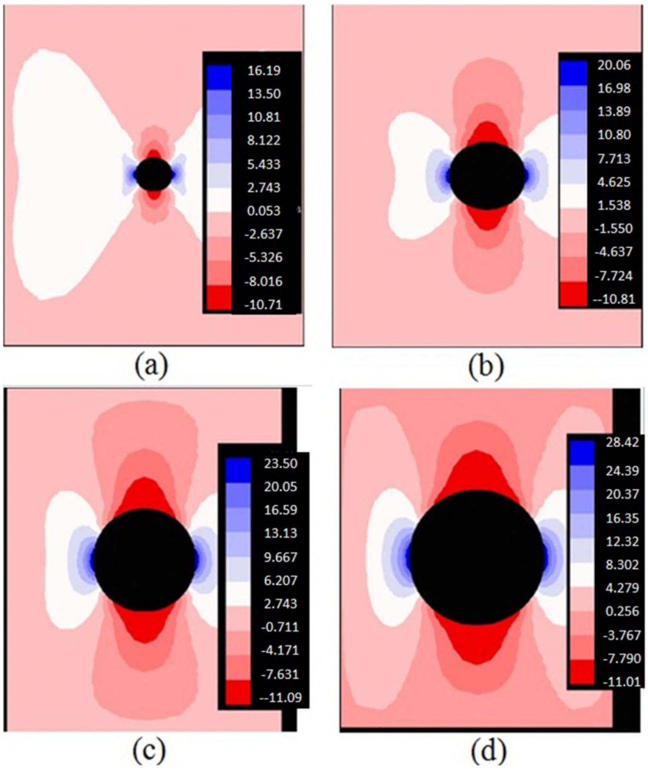

Fig. 11 Tensile stress distribution in the samples when W/B is (a) 0.125, (b) 0.25, (c) 0.375, (d) 0.5

crack growth process are specified. Fig. 10 shows finite mesh with boundary and loading conditions. Up and down sides of the model were fixed in *x* direction and the left and the right sides were fixed in *y* direction. To obtain detailed distribution of induced stresses up to 400 elements have been used in the models. In the simulations, specimens with four different *W/B* ratios; 0.15, 0.25, 0.375, and 0.5; were used. Where, *W* is the diameter of the hole and *B* is the widths of sample. These models were subjected under internal tensile stress of 10 MPa. The analyses were made on samples assuming that the concrete is linearly elastic and isotropic. The elastic modulus and Poisson's ratio for the specimens used in the model measured by uniaxial compression test were 25 GPa and 0.20, respectively.

The objective of model analyses was to verify that the failure under tensile loading occurs at the mid-length. No compressive stress exists at the mid-length of the specimen. The specimen fails under tensile loading before the failure by shear stress occurs at both ends of specimen. Fig. 11 shows stress distribution in the samples for different ratios of the hole diameter to the sample width. This figure shows concentrated tensile stress at the left and the right sides of the hole. The compressive stress is also concentrated at top and bottom of the hole. Generally the tensile strength of concrete is less than its compressive strength; therefore the sample fails along the horizontal axes of the hole on both sides before any failure can happen under any compression loading vertically.

Fig. 12 shows distribution of the normalized tensile stress (S2) and shear stress (S) by far field failure stress (Pt) versus horizontal distance from the center of hole. Maximum shear and tensile

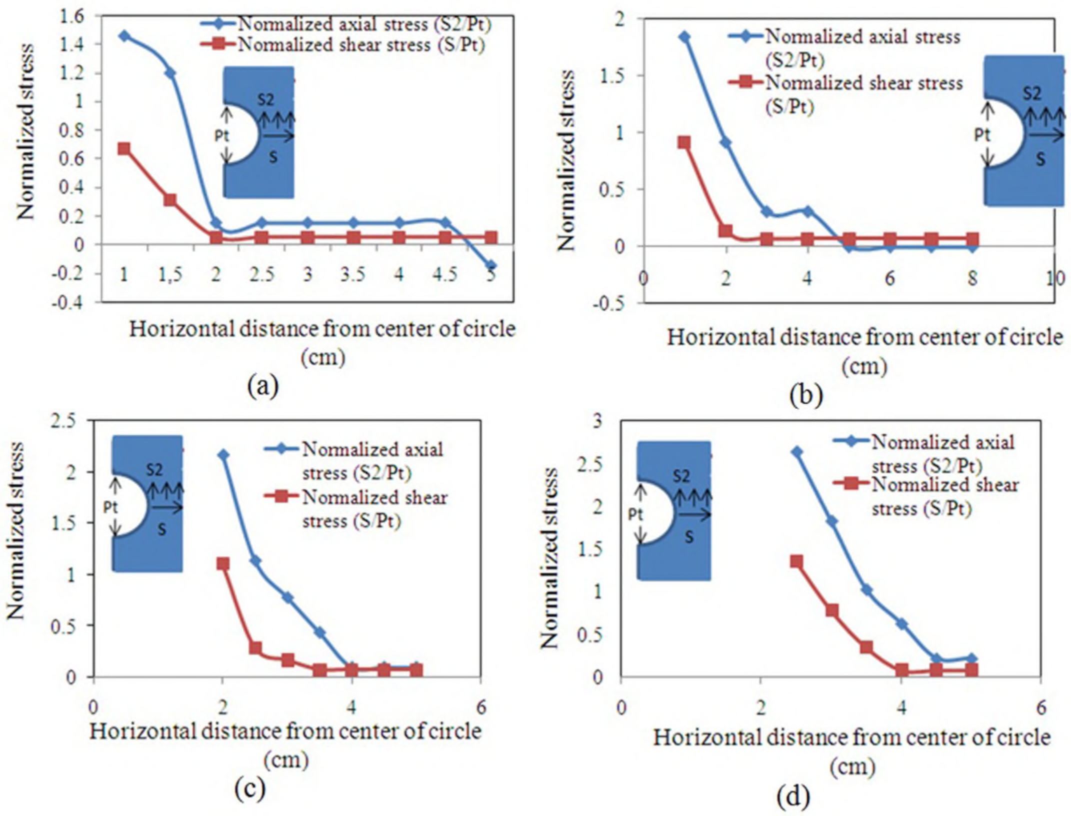

Fig. 12 The variation of normalized stress versus horizontal distance from hole center; the ratio of hole diameter to sample width is (a) 0.125, (b) 0.25, (c) 0.375 (d) 0.5

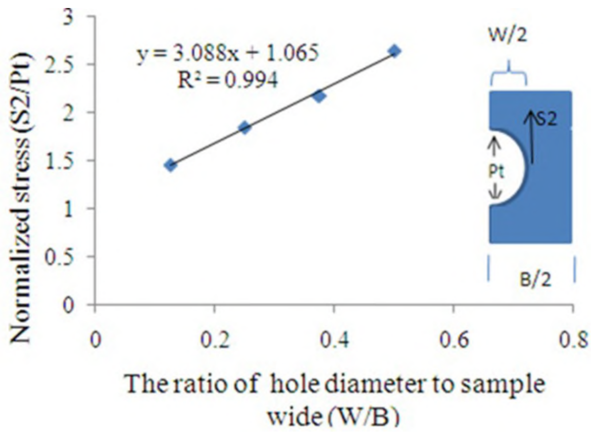

Fig. 13 The variation of normalized tensile stress concentration (S2/Pt) vs the ratio of hole's diameter to the sample's width (W/B)

stresses occur near the applied loading areas. Also, the value of tensile stress in the side of the hole is more than shear stress in all samples. Whereas the tensile strength of material is less than its

Table 2 Results of indirect tensile strength in three different directions

Sample No. (*W/B*=0.5)	Tensile strength (MPa) when vertical sides of sample are parallel to the loading axis	Tensile strength (MPa) when vertical sides of sample are returned 45° non counter clock wise related to the loading direction	Tensile strength (MPa) when vertical sides of sample are returned 45° counter clock wise related to the loading direction
1	3.1	3.16	3.19
2	3.08	3.2	3.21
Average	3.09	3.18	3.2

shear strength, therefore these models have tensile failure in the side of the hole of specimen before any failure under shear loading in centerline. It can be concluded from the numerical analysis results that, the model with internal hole would be suitable for the use in compression-to-tension load transformer (CTT). Whereas concentration of tensile stress in the model is more than the far field tensile stress, therefore the far field tensile stress could not be used directly as tensile strength of concrete slab. For determination of the real tensile strength of concrete slab, the relationship between concentrated tensile stress, far field tensile stress and hole diameter should be specified.

Fig. 13 shows the variation of normalized tensile stress concentration on the hole along the horizontal axis in relation to the ratio of hole diameter to sample width.

The regression equation (i.e., Eq. (1)) can be used to predict S2/Pt for any *W/B* ratio between 0.125 and 0.5.

$$S2/Pt=3(W/B)+1 \tag{1}$$

This equation shows that, when far field failure stress (*Pt*) was applied to a solid specimen or one with a very small hole (*W*~0), the tensile stress concentration along the horizontal axes of the hole on both sides (S2) is equal to *Pt*. This means that, internal stresses in a fine hole act similar to the point loading with constant stress around the hole. The stress concentration around the hole increases by increasing the hole diameter (Fig. 10). This finding is in a good accordance with Kirsch solution results (Brady 2006).

S2 can be calculated using Eq. (1) by substituting the *Pt*. When the far field failure stress of 1.24 MPa (*Pt* from the test) was applied on sample with the ratio of *W/B*=0.5, S2 calculated to 3.1 MPa. Therefore, 3.1 MPa was the ultimate tensile strength of sample. Table 2 shows a comparison of tensile strength of concrete for three different directions.

2.6 Comparison of the strength results

Table 2 compares the tensile strengths of concrete determined from three different loading directions. The anisotropic tensile strengths of concrete nearly were similar due to homogeneity of bonding between concrete materials and also due to randomly accumulation of weak plane in concrete mortar.

Also, Table 3 compares the tensile strength results obtained from three methods. The Splitting tension test yields the highest strength values due to the high stress gradient along the incipient crack plane (Zain *et al*. 2002). It is interesting to note that the difference between the Splitting and

Table 3 Results of direct tensile strength in three different directions

Sample NO.	In direct tensile strength (MPa)	Splitting tensile strength (MPa)	Three point tensile strength (MPa)
1	3.09	4.2	3.4
2	3.18	4.1	3.4
3	3.2	4.07	3.2
Average	3.15	4.1	3.33

direct tensile strengths is about 30%. Also, the difference between the three point and direct tensile strengths is about 5.7%. The difference of the tensile strength from the three methods may therefore be partly governed by tensile stress distribution on the failure surface.

3. Conclusions

The CTT device was designed to obtain anisotropic tensile strengths of concrete under uniaxial tensile and to induce extension failure under a true uniaxial tensile stress. The hole diameter at the mid-section of specimen was 75 mm, which may raise the influence of hole size on the measured strength. The effect of hole size on tensile strength of a concrete tensile strength was determined using numerical simulation. It has been concluded that, as the hole size increases, the tensile stress concentration in the side of the hole along the horizontal axis increases under a constant far field stress. The real concrete tensile strength is calculated based on Eq. (1). It is recognized here that the anisotropic tensile strengths of concrete nearly are similar due to homogeneity of bonding between concrete materials and also due to randomly accumulation of weak plane in concrete mortar. It should be recognized here that, the indirect tensile strength was lower than the Brazilian tensile strength and three point tensile strength.

CTT can be used for testing on other concrete mix designs but because of having limitation in installing the CTT device, the minimum practical hole size should be 75 mm.

References

Brady, B.H.G. and Brown E.T. (2006), *Concrete Mechanics for Underground Mining*, 3rd Edition, Chapman & Hall, London.

BS1881-117 (1983), *Testing Concrete - Method for determination of tensile splitting strength*, British Standards Institute, London.

BS1881-118 (1983), *Testing Concrete - Method for determination of flexural strength*, British Standards Institute, London, U.K.

Calixto, J.M.F. (2002), “Experimental investigation of tensile behavior of high strength concrete”, *Mater. Res. J.*, **5**(3), 295-303.

Gerges, N.N., Issa, C.A. and Fawaz, S. (2015), “Effect of construction joints on the splitting tensile strength of concrete”, *Case Studies Constr. Mater.*, **3**, 83-91.

Gomez, J.T., Shukla, A. and Sharma, A. (2001), “Static and dynamic behavior of concrete and granite in tension with damage”, *Theor. Appl. Fract. Mech.*, **36**(1), 37-49.

Kim, J.J. and Reda Taha, M. (2014), “Experimental and numerical evaluation of direct tension test for cylindrical concrete specimens”, *Adv. Civil Eng.*, **2014**, 8

Larrard, F, Malier, Y. (1992), *Engineering Properties of Very High Performance Concrete*, Ed. Malier, Y., High Performance Concrete, From Material to Structure, London.

Liu, X., Nie, Z., Wu, S. and Wang, C. (2015), "Self-monitoring application of conductive asphalt concrete under indirect tensile deformation", *Case Studies Constr. Mater.*, **3**, 70-77.

Van Mier, J.G.M. and Van Vliet, M.R.A. (2002), "Uniaxial tension test for the determination of fracture parameters of concrete: state of the art", *Eng. Fract. Mech.*, **69**(2), 235-247.

Mobasher, B., Bakhshi, M. and Barsby, C. (2014), "Backcalculation of residual tensile strength of regular and high performance fiber reinforced concrete from flexural tests", *Constr. Build. Mater.*, **70**, 243-253.

Swaddiwudhipong, S., Lu, H.R. and Wee, T.H. (2003), "Direct tension test", *Cem. Concr. Res.*, **33**, 2077-2084.

Silva, R.V., De Brito, J. and Dhir, R.K. (2015), "Tensile strength behaviour of recycled aggregate concrete", *Constr. Build. Mater*., **83**, 108-118.

Tian, Y., Shi, S., Jia, K. and Hu, S. (2015), "Mechanical and dynamic properties of high strength concrete modified with lightweight aggregates presaturated polymer emulsion", *Constr. Build. Mater*., **93**, 1151-1156.

Ibrahim, M.W., Hamzah, A.F., Jamaluddin, N., Ramadhansyah, P.J. and Fadzil, A.M. (2015), "Split tensile strength on self-compacting concrete containing coal bottom ash", *Procedia-Social Behav. Sci.*, **195**, 2280-2289.

Wawrzynek, P.A. and Ingraffea, A.R. (1987), "Interactive finite element analysis of fracture processes: an integrated approach", *Theor. Appl. Fract. Mech.*, **8**(2), 137-150.

Zain, M.F.M., Mahmud, H.B., Ilham, A. and Faizal, M. (2002), "Splitting tensile strength of high-performance concrete", *Cement Concrete Res.*, **32**, 1251-1257.

Zheng, W., Kwan, A.K.H. and Lee, P.K.K. (2001), "Direct tension test of concrete", *Mater. J.*, **98**(1), 63-71.

Zhou, F.P. (1988), *Some aspects of tensile fracture behaviour and structural response of cementitious materials*, Report TVBM 1008.

CC